THE JOURNAL OF BIOLOGICAL CHEMISTRY
Vol. 276, No. 43, Issue of October 26, pp. 40241–40246, 2001

*Printed in U.S.A.*

# Natural Osmolyte Trimethylamine *N*-Oxide Corrects Assembly Defects of Mutant Branched-chain α-Ketoacid Decarboxylase in Maple Syrup Urine Disease*

Received for publication, July 30, 2001
Published, JBC Papers in Press, August 15, 2001, DOI 10.1074/jbc.M107242200

**Jiu-Li Song and David T. Chuang‡**

*From the Department of Biochemistry, University of Texas Southwestern Medical Center, Dallas, Texas 75390-9038*

**Maple syrup urine disease is caused by deficiency in the mitochondrial branched-chain α-ketoacid dehydrogenase (BCKD) complex. The clinical phenotype includes often fatal ketoacidosis, neurological derangement, and mental retardation. The type IA mutations Y393N-α, Y368C-α, and F364C-α, which occur in the E1α subunit of the decarboxylase (E1) component of the BCKD complex, impede the conversion of an αβ heterodimeric intermediate to a native $\alpha_2\beta_2$ heterotetramer in the E1 assembly pathway. In the present study, we show that a natural osmolyte trimethylamine *N*-oxide (TMAO) at the optimal 1 M concentration restores E1 activity, up to 50% of the wild type, in the mutant E1 carrying the above missense mutations. TMAO promotes the conversion of otherwise trapped mutant heterodimers to active heterotetramers. This slow step does not involve dissociation/reassociation of the mutant heterodimers, which are preformed in the presence of chaperonins GroEL/GroES and Mg-ATP. The TMAO-stimulated mutant E1 activity is remarkably stable upon removal of the osmolyte, when cofactor thiamine pyrophosphate and the transacylase component of the BCKD complex are present. The above *in vitro* results offer the use of chemical chaperones such as TMAO as an approach to mitigate assembly defects caused by maple syrup urine disease mutations.**

Maple syrup urine disease (MSUD)[1] or branched-chain ketoaciduria is an autosomal recessive metabolic disorder in the catabolism of branched-chain α-ketoacids derived from leucine, isoleucine, and valine (1). The accumulated branched-chain α-ketoacids and amino acids are secreted in the urine, giving rise to a distinct maple syrup odor and hence the name of the disease (2). Based on the clinical presentation and biochemical responses to thiamine treatment, MSUD can be grouped into five distinct phenotypes, classic, intermediate, intermittent, thiamine-responsive, and dihydrolipoamide dehydrogenase (E3)-deficient forms (1). Classic MSUD has a neonatal onset of often fatal ketoacidosis and encephalopathy, which lead to mental retardation in survivors. Intermediate and intermittent forms show milder symptoms with a late onset. Patients with thiamine-responsive MSUD respond to pharmacological doses of thiamine with returns to the normal levels of branched-chain amino acids (3). Patients with E3 deficiency have combined enzyme impairments in α-ketoacid dehydrogenase complexes and usually die in infancy with severe lactic acidosis (4). The prevalence of MSUD is 1 in 185,000 newborns worldwide, but in certain populations, for example the Mennonites, the incidence is as high as 1 in 176 life births, as a result of consanguinity.

The enzyme affected in MSUD, the mitochondrial branched-chain α-ketoacid dehydrogenase (BCKD) complex, is a multienzyme complex of 4–5 million daltons. It is organized about a 24-meric cubic core of dihydrolipoyl transacylase (E2). Attached to the E2 core are multiple copies of branched-chain α-ketoacid decarboxylase (E1), E3, BCKD kinase, and BCKD phosphatase (5, 6). The kinase and the phosphatase tightly regulate activity of the BCKD complex by reversible phosphorylation (inactivation)/dephosphorylation (activation) (7). The E1 component is a thiamine pyrophosphate (TPP)-dependent enzyme consisting of two α and two β subunits. The E3 component is a homodimeric flavoprotein and is common in the family of mitochondrial α-ketoacid dehydrogenase complexes comprising pyruvate dehydrogenase, α-ketoglutarate dehydrogenase, and BCKD complexes. Therefore, MSUD is genetically heterogeneous, and mutations in four (E1α, E1β, E2, and E3) of the six subunits that comprise the BCKD complex have been reported in affected patients (1). On the basis of the affected subunit in the BCKD complex, MSUD is classified into six genetic subtypes (1). Among them, type IA MSUD affects the E1α subunit, type IB the E1β subunit, type II the E2 subunit, and type III the E3 subunit. Type IV and type V MSUD involve the kinase and the phosphatase, respectively, in which the disease-causing mutations have not been detected.

The crystal structure of the human E1 $\alpha_2\beta_2$ heterotetramer was determined recently to 2.7-Å resolution (8). The overall $\alpha_2\beta_2$ heterotetrameric structure dictates that each subunit is in contact with the other three subunits. Subunits α, α′, β, and β′ are designated such that the α and the β subunits when combined correspond to one polypeptide of the related dimeric yeast transketolase (9) and are equivalent to the αβ heterodimeric assembly intermediate of human E1 (10). Each of the two binding sites for cofactor TPP is located in the interface between α and β subunits. The E1 structure also discloses that the extended small C-terminal region protruding from the bulk of the E1α subunit is essential for the interaction between heterologous α and β subunits. This segment is referred to as the "Mennonite" region, because it contains the type IA Y393N-α mutation, which is prevalent in the Mennonite pop-

* This work was supported by Grant DK-26758 from the National Institutes of Health and Grant I-1286 from the Robert A. Welch Foundation. The costs of publication of this article were defrayed in part by the payment of page charges. This article must therefore be hereby marked "*advertisement*" in accordance with 18 U.S.C. Section 1734 solely to indicate this fact.

‡ To whom correspondence should be addressed. Tel.: 214-648-2457; Fax: 214-648-8856; E-mail: David.Chuang@UTSouthwestern.edu.

[1] The abbreviations used are: MSUD, maple syrup urine disease; BCKD, branched-chain α-ketoacid dehydrogenase; DTT, dithiothreitol; E1, branched-chain α-ketoacid decarboxylase; E2, dihydrolipoyl transacylase; E3, dihydrolipoamide dehydrogenase; NTA, nitrilotriacetic acid; TMAO, trimethylamine *N*-oxide; TPP, thiamine pyrophosphate; TEV, tobacco etch virus.

ulation (11, 12). The Tyr to Asn mutation at position 393 of the $\alpha$ subunit abrogates the interaction between $\alpha$ and $\beta'$ subunits and prevents chaperonin GroEL/GroES-dependent heterotetramer assembly, with the mutant E1 locked in an ensemble of inactive heterodimeric conformations (10). The other two type IA mutations in the Mennonite region, F364C-$\alpha$ and Y368C-$\alpha$, also disrupt the heterologous $\alpha$ and $\beta'$ and $\alpha$ and $\beta$ subunit interactions, respectively, resulting in the inability to assemble into the native heterotetrameric conformation.

Naturally occurring osmolyte trimethylamine *N*-oxide (TMAO) is present in high concentrations in coelacanth (sharks) and marine elasmobranchs (rays) (13). It counteracts the damaging effects of concentrated urea on protein folding and stability in these organisms (14). This osmolyte has been shown to force the *in vitro* folding of normally unstructured proteins such as glucocorticoid receptor 1–500-amino acid fragments and AF1/tau1 domain (15, 16) and reduced/carboxyamidated ribonucleases (17, 18). TMAO has also been reported to increase the folding efficiency of a truncated glutamine synthetase (19). TMAO is shown to correct temperature-sensitive folding defects of ΔF508 in cystic fibrosis transmembrane conductance regulator (20), and interfere with the formation of scrapie prion protein (21), but not to increase the secretion of mutant $\alpha$-antitrypsin Z (22). Studies to date have focused on the positive effects of TMAO on protein folding, which is apparently mediated via a solvophobic mechanism, resulting from unfavorable interactions between the osmolyte and the peptide backbones (18).

In this study, we employed TMAO as a possible chemical chaperone (23) to ameliorate the MSUD phenotype caused by mutations in the E1 components of the BCKD complex. We report that TMAO significantly augments residual E1 activity in the above type IA MSUD mutants associated with E1 assembly defects. Interestingly, the activation occurs after mutant E1 has been folded and misassembled. TMAO corrects the assembly defects in MSUD mutants by promoting the conversion of trapped mutant heterodimers to active heterotetramers. This is the first report of the positive effect of TMAO in correcting protein assembly defects caused by human mutations.

## EXPERIMENTAL PROCEDURES

*Expression and Purification of Recombinant Wild Type and MSUD Mutant E1*—The Altered Site *in vitro* mutagenesis system from Promega (Madison, WI) was used to introduce desired known MSUD mutations into the cDNA for the E1$\alpha$ or E1$\beta$ subunit. Detailed protocols for the mutagenesis and the construction of the pHis-TEV-E1 plasmid coexpressing wild type or mutant human E1$\alpha$ and E1$\beta$ subunits were described previously (24). These expression vectors contained a $His_6$ tag linked (5′ to 3′) to the TEV protease site, followed by the N terminus of the E1$\alpha$ subunit, and the E1$\beta$ subunit was untagged. The pHis-TEV-E1 plasmid and the pGroESL plasmid overexpressing bacterial chaperonins GroEL/GroES were cotransformed into *Escherichia coli* CG-712 $ES^{ts}$ cells, and recombinant $His_6$-tagged E1 wild type and mutant proteins were expressed and purified as described previously (10, 25, 26). E1 activity was assayed either radiochemically (27) or spectrophotometrically (28), based on the reconstituted BCKD activity in the presence of excess E2 and E3. Protein concentrations were determined using Coomassie Blue Plus from Pierce with bovine serum albumin as standard.

*Incubation of MSUD Mutant E1 Proteins with TMAO*—The 4 M stock solution of TMAO (from Sigma) was prepared by dissolving 44.44 g of TMAO in distilled water to a final volume of 100 ml. The stock solution was filtered through a 0.2-$\mu$m membrane filter and stored at room temperature. Mutant E1 proteins (200 $\mu$g/ml) were incubated with different concentrations of TMAO at 23 °C for 16 h in Buffer A, comprising 50 mM potassium phosphate, pH 7.5, 100 mM KCl, 2 mM TPP, 2 mM $MgCl_2$, 10 mM dithiothreitol (DTT), and the Complete protease inhibitor mixture (Roche Molecular Biochemicals). Aliquots taken at different times or at the end of the incubation were analyzed for E1 activity and protein concentration.

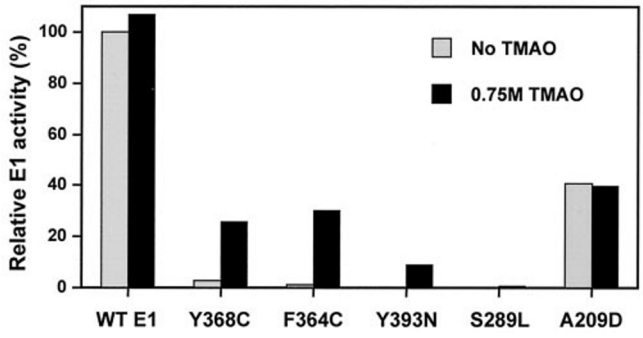


FIG. 1. **TMAO restores enzyme activity of mutant E1 carrying MSUD mutations.** Wild type (*WT*) E1 and various mutant E1 were incubated with Buffer A (see "Experimental Procedures") with or without 0.75 M TMAO at 23 °C for 16 h. E1 activity was measured radiochemically based on reconstituted BCKD activity in the presence of E2 and E3. The activity of 1 $\mu$g of wild type E1 in the absence of TMAO was set as 100%.

*Sucrose Density Gradient Analysis of TMAO-treated Mutant E1*—Mutant E1 at 200 $\mu$g/ml was incubated with 0.75 M TMAO in Buffer A for 16 h at 23 °C. After centrifugation, the supernatant was applied to a 10-ml 10–25% sucrose density gradient containing 0.75 M TMAO and was spun at 210,000 × *g* for 18 h at 4 °C. As a control, wild type E1 also in Buffer A was separated on an identical sucrose gradient with 0.75 M TMAO in the same run. Untreated wild type and mutant E1 proteins were separated on a 15–30% sucrose gradient in the absence of TMAO. The wild type E1 heterotetramer sedimented to the same position on both gradients. Aliquots of the fractions collected from top to bottom were analyzed by SDS-polyacrylamide gel electrophoresis after trichloroacetic acid precipitation. The remaining aliquots were assayed radiochemically for E1 activity after precipitation with 65% (w/v) ammonium sulfate.

*In Vitro Refolding of Wild Type and Mutant E1 in the Presence of TMAO*—Wild type and mutant E1 were denatured for 1 h at 23 °C in 8 M urea in a buffer containing 50 mM potassium phosphate, pH 7.5, 100 mM KCl, and 10 mM DTT to make a final protein concentration of 2 mg/ml (12.5 $\mu$M E1 heterotetramer). Denatured E1 was rapidly diluted 100-fold on a Vortex mixer into Buffer A containing 1 $\mu$M GroEL (14-mer), 2 $\mu$M GroES (7-mer), followed by the addition of different concentrations of TMAO. The refolding was initiated with 10 mM Mg-ATP added to the refolding mixture. After incubation at 23 °C for 16 h, E1 proteins in the refolding mixture were precipitated with 65% ammonium sulfate. The protein pellet was redissolved in 50 $\mu$l of Buffer A and analyzed for recovered E1 activity by the radiochemical assay.

*CD Spectroscopy*—CD spectra of wild type and MSUD mutant E1 proteins were recorded at 25 °C in an Aviv 62DS spectropolarimeter using a 1.0-mm cuvette, with a bandwidth of 1.5 nm and scan step of 1 nm. Spectra were recorded at a protein concentration of 0.2 mg/ml in 50 mM potassium phosphate, pH 7.5, 100 mM KCl, 0.5 mM DTT, and 0.5 mM EDTA. Each spectrum was an average of three consecutive scans from 260 to 190 nm and was corrected for contributions from the buffer solution.

## RESULTS

*Activation of MSUD Mutant E1 by TMAO Treatment*—We selected for study five MSUD mutations that affect the E1 component of the BCKD complex. The Y368C-$\alpha$, F364C-$\alpha$, and Y393N-$\alpha$ type IA mutations that are located in the C-terminal region of the E1$\alpha$ subunit produce severe classic phenotype. An additional type IA mutation A209D-$\alpha$ shows significant residue activity and is present in a compound-heterozygous Caucasian patient with an intermediate MSUD phenotype. A single type IB mutation S289L-$\beta$, which is prevalent in the Israeli Druze kindred, also gives rise to the classic MSUD phenotype (29). Fig. 1 shows that 0.75 M TMAO has no significant effect on wild type E1 activity, with activity in the absence of TMAO set as 100%. In contrast, activity of F364C-$\alpha$ mutant E1 was increased markedly from 1% of wild type without TMAO to 30% with 0.75 M TMAO. Similar effects were obtained with Y368C-$\alpha$ E1 in that residue activity is 3% in the absence of TMAO and 27% in its presence. TMAO also activated Y393N-$\alpha$ E1 with

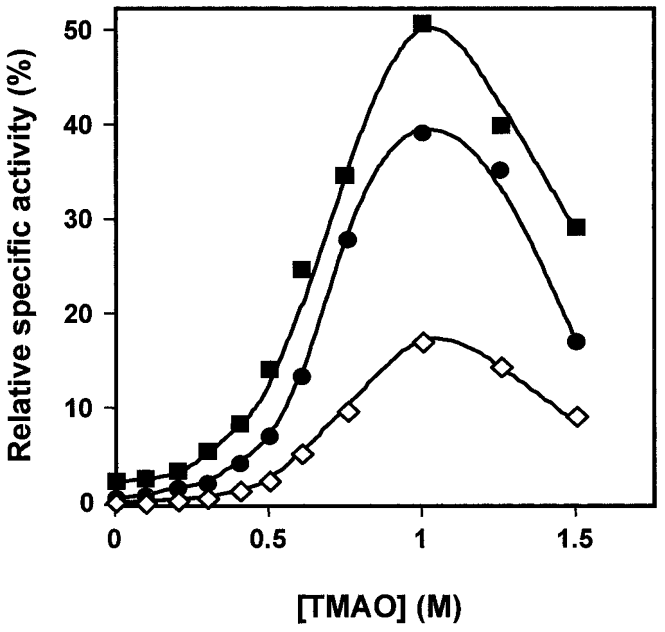


FIG. 2. **The optimal stimulation of MSUD mutant E1 occurs at 1 M TMAO concentration.** Y368C-$\alpha$ (■), F364C-$\alpha$ (●), and Y393N-$\alpha$ (◇) mutant E1 at 0.2 mg/ml were incubated in Buffer A (see Fig. 1) with different concentrations of TMAO at 23 °C for 16 h. After centrifugation at 12,000 rpm at 4 °C for 10 min, aliquots were taken from the supernatant for radiochemical E1 activity assay and protein concentration determination. Specific activity was calculated for each sample and expressed as a percentage of the specific activity of wild type E1.

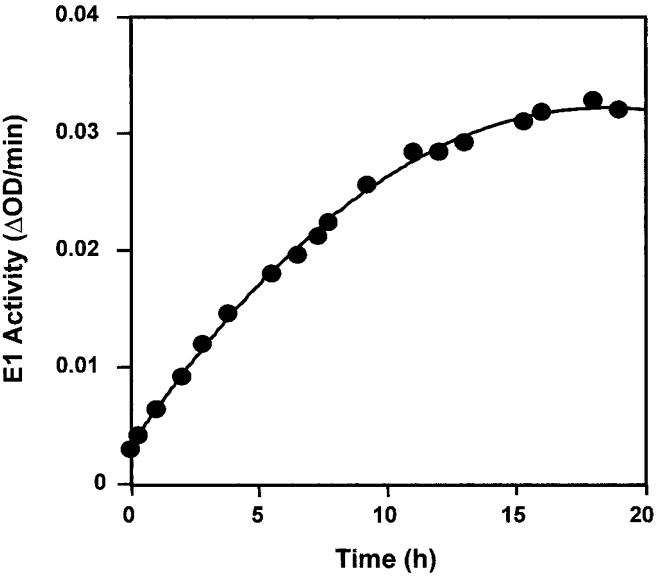


FIG. 3. **TMAO-mediated activation of MSUD mutant E1 is a slow process.** Y368C-$\alpha$ mutant E1 was added into Buffer A (see Fig. 1) containing 1 M TMAO at 23 °C to a final concentration of 0.2 mg/ml. Aliquots of 50 $\mu$l taken at different times during the incubation were assayed for E1 activity spectrophotometrically based on reconstituted BCKD complex activity. The activity of Y368C-$\alpha$ mutant E1 before the incubation with TMAO was set as activity at the zero time. $\Delta OD$, change of absorbance at 340 nm.

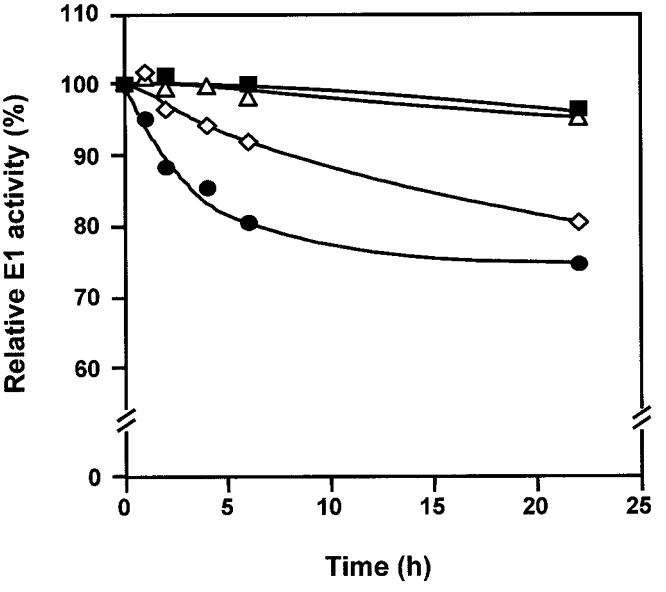


FIG. 4. **TMAO-rescued mutant E1 activity is stable upon removal of the osmolyte.** Y368C-$\alpha$ mutant E1 was activated by incubating with 1 M TMAO in Buffer A (see Fig. 1) at 23 °C for 16 h. After centrifugation at 12,000 rpm for 10 min, the supernatant was diluted 10-fold into the E1 spectrophotometrical assay mixture (■) or the assay mixture without E2 (●), TPP (◇), or DTT (△), followed by incubation at 23 °C. At the indicated time, aliquots of 500 $\mu$l were taken and incubated at 30 °C. After 2 min, 2 mM $\alpha$-ketoisovalerate (substrate) and the deleted component (E2, TPP, or DTT) were added to the incubation mixture to initiate the enzyme assay. The activity of same amount of Y368C-$\alpha$ mutant E1 before dilution was set as 100%.

activity increased from 0 to 9% of the wild type, in the absence and the presence of TMAO, respectively. The S289L-$\beta$ and A209D-$\alpha$ mutants showed 0 and 40% residual activities, respectively, in the absence of TMAO, but these activities remained unchanged after incubation with the osmolyte.

The activation of MSUD E1 mutants by TMAO treatment was studied further by titrating the osmolyte concentration. Fig. 2 shows that the activation of E1 activity for the three type IA MSUD mutants Y368C-$\alpha$, F364C-$\alpha$, and Y393N-$\alpha$ is insignificant below 0.4 M TMAO. Rapid rises in residual E1 activity were obtained at 0.5 M or higher TMAO concentrations. The highest degree of activation occurs at 1 M TMAO concentration for all three MSUD mutants, with Y368C-$\alpha$ at 50%, F364C-$\alpha$ at 39%, and Y393N-$\alpha$ at 17% of the wild type specific activity. At higher than 1 M TMAO concentrations, elevated residual E1 activities decline precipitously.

*Kinetics and Stability of TMAO Activation*—The time course of TMAO activation was investigated with Y368C-$\alpha$ E1 in the presence of 1 M TMAO. As shown in Fig. 3, the TMAO-mediated activation of the mutant E1 is a slow process. The activation curve reached a plateau at 18 h, with a $t_{1/2}$ of 5 h. The TMAO-augmented Y368C-$\alpha$ E1 activity, after a 10-fold dilution in the complete activity assay mixture, was completely stable in 4 h and declined only slightly to 95% of the zero time after incubation for 22 h at 23 °C (Fig. 4). Similar results were obtained when DTT was omitted from the incubation mixture. In the absence of TPP, activity of the TMAO-stimulated Y368C-$\alpha$ mutant E1 declined gradually to 80% at 22 h. When E2 was depleted from the incubation mixture, a steeper decrease in stimulated E1 activity occurred, which reached 80% of the zero time at 6 h and 75% at 22 h. The above data indicate that both E2 and TPP are required to optimally stabilize TMAO-stimulated activity of the mutant E1.

*TMAO Corrects Assembly Defects of MSUD Mutant E1*—It was shown previously that type IA mutations Y393N-$\alpha$, F364C-$\alpha$, and Y368C-$\alpha$ impede heterotetrameric assembly in mutant E1 (10). We therefore investigated the possible effect of TMAO on mutant E1 assembly. The Y393N-$\alpha$ Mennonite mutation leads to trapped inactive heterodimers, which migrated near the top of the sucrose density gradient and peaked at fraction 3 (Fig. 5*A*). After a 16-h incubation with 0.75 M TMAO at 23 °C, the Y393N-$\alpha$ mutant E1 sedimented as a heterotetramer and peaked at fraction 5, similar to wild type E1 without

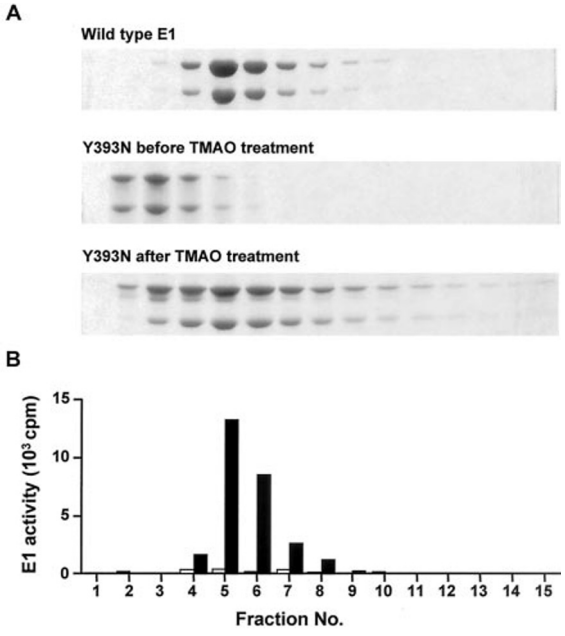


FIG. 5. **TMAO promotes the conversion of trapped mutant E1 heterodimers to heterotetramers to restore E1 activity.** *A*, sucrose density gradient analysis of wild type and mutant E1. The Y393N-$\alpha$ mutant E1 before and after 0.75 M TMAO treatment was separated by sucrose density gradient centrifugation as described under "Experimental Procedures." Wild type E1 without TMAO treatment was run concurrently as a control. *B*, E1 activity profile of the sucrose density gradient fractions. E1 activity of each fraction was assayed radiochemically as described in the legend for Fig. 1. *Open bars*, Y393N-$\alpha$ mutant E1 before TMAO treatment; *filled bars*, after TMAO treatment.

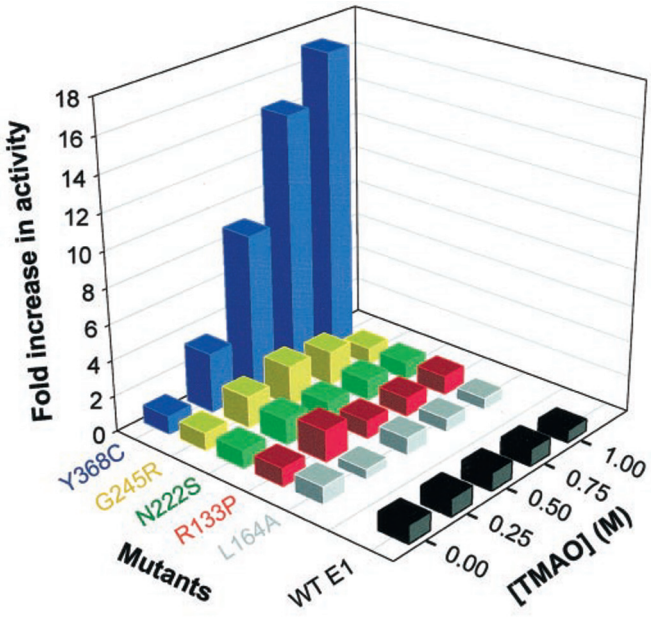


FIG. 6. **TMAO markedly enhances mutant E1 activity renatured in the presence of chaperonins GroEL/GroES.** Urea-denatured wild type (*WT*) and mutant E1 were refolded in a buffer containing chaperonin GroEL/GroES and different concentrations of TMAO as described under "Experimental Procedures." After incubation at 23 °C for 16 h, recovered E1 activity was measured by the radiochemical assay. Activity recovered in the absence of TMAO is set as 1.0.

TMAO treatment. Fractions that contained Y393N-$\alpha$ heterodimers prior to TMAO incubation did not exhibit E1 activity (Fig. 5*B*). The conversion from $\alpha\beta$ heterodimers to $\alpha_2\beta_2$ heterotetramers after TMAO treatment coincided with the presence of E1 activity in the sucrose density gradient fractions (fractions 4–7). Similar results were obtained with F364C-$\alpha$ and Y368C-$\alpha$ mutant E1. The data provide direct evidence that TMAO corrects assembly defects in MSUD by promoting the conversion of trapped inactive heterodimers into active heterotetramers.

*TMAO Activates Mutant E1 during Chaperonin-mediated Refolding*—The above results show that TMAO augments residual activity of folded MSUD mutant E1. Here, we further decipher the effect of TMAO on mutant E1 activity during GroEL/GroES-mediated folding (Fig. 6). TMAO efficiently stimulated activity recovery of the Y368C-$\alpha$ mutant E1 in an osmolyte concentration-dependent manner. The highest degree of reactivation, which showed 17-fold increase over baseline activity (no osmolyte), was obtained at 1 M TMAO concentration. A smaller but significant activation was observed with the G245R-$\alpha$ mutant E1, with a maximal 2.5-fold increase over the baseline at 0.5 M TMAO. Insignificant activation by TMAO was obtained with N222S-$\alpha$, R133P-$\beta$, and L164A-$\alpha$ mutant E1. Refolded wild type E1 activity was unchanged in the presence or absence of TMAO.

We showed previously that chaperonins GroEL/GroES promote the conversion of wild type E1 heterodimers to heterotetramers through a dissociation/reassociation cycle (30, 31). To address whether TMAO induced dissociation of mutant assembly intermediates, the Y368C-$\alpha$ E1, which comprised predominantly trapped heterodimers with a $His_6$ tag on the E1$\alpha$ subunit, was immobilized on $Ni^{2+}$-NTA resin and incubated with GroEL with or without 0.75 M TMAO. TMAO-induced dissociation of the mutant heterodimer would have triggered the release of the untagged E1$\beta$ subunit from the resin to be trapped by GroEL in the supernatant. Fig. 7 showed that a GroEL-$\beta$ complex was not detected in the supernatant after removal of the resin by centrifugation, either in the presence or the absence of TMAO. The stoichiometry of E1$\alpha$:E1$\beta$ was maintained at 1:1 either in the presence and the absence of TMAO, irrespective of the addition of GroEL, in the eluted fractions. The data, taken together, indicate that the mutant heterodimers immobilized on $Ni^{2+}$-NTA resin did not undergo dissociation into individual E1$\alpha$ and E1$\beta$ subunits. Minor top bands in the fractions eluted from the $Ni^{2+}$-NTA resin represented nonspecific binding of GroEL.

*Secondary Structures of Wild Type E1 and MSUD Mutant E1*—Wild type E1 and F364C-$\alpha$, Y368C-$\alpha$, and Y393N-$\alpha$ mutant E1 proteins were analyzed by CD spectroscopy. As shown in Fig. 8, all spectra are very similar, with one maximum at 195 nm and two minima at 208 and 220 nm. The 220-nm minimum might be because of the combination of $\alpha$-helix (peak at 222 nm) and $\beta$-sheet (peak at 218 nm) structures. The overall secondary structures of the wild type and the three mutant E1 are very similar. However, Y393N-$\alpha$ and F364C-$\alpha$ E1 appear to have a slightly higher content of secondary structures, compared with the wild type E1 and the Y368C-$\alpha$ mutant E1.

## DISCUSSION

The MSUD mutations studied here, Y393N-$\alpha$, Y368C-$\alpha$, and F364C-$\alpha$, involve three aromatic residues that are critical for the packing of the C-terminal region of the E1$\alpha$ subunit against the heterologous E1$\beta'$ or E1$\beta$ subunit (Fig. 9). The Tyr-393-$\alpha$ residue is hydrogen-bonded to His-385-$\alpha$ and Asp-328-$\beta'$ in the E1$\alpha$ and E1$\beta'$ subunits, respectively (8). A Tyr to Asn conversion in the Mennonite Y393N-$\alpha$ mutation impedes the $\alpha/\beta'$ subunit interaction necessary for the cross-talk between $\alpha\beta$ and $\alpha'\beta'$ heterodimers. This prevents $\alpha_2\beta_2$ heterotetrameric assembly of native E1, resulting in permanently trapped heterodimers. The side chain of the Phe-364-$\alpha$ residue in the E1$\alpha$ subunit is packed tightly against the side chain of Tyr-313-$\beta'$ in the E1$\beta'$ subunit. The F364C-$\alpha$ mutation is likely to also affect

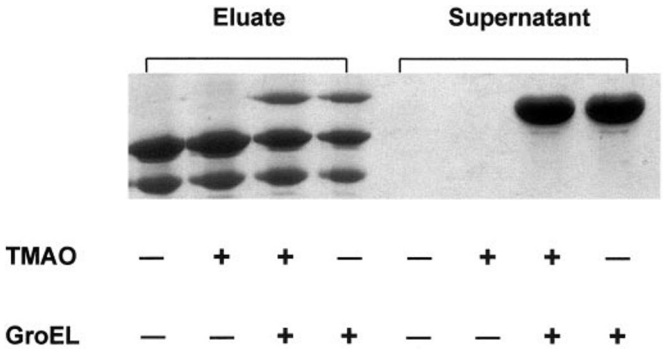


FIG. 7. **The mutant heterodimeric intermediate does not undergo dissociation in the presence of TMAO.** Y368C-$\alpha$ mutant E1 was immobilized on $Ni^{2+}$-NTA resin by incubation at 4 °C for 2 h. After washing with Buffer A (see Fig. 1), the resin was divided into four aliquots. The aliquots were incubated at 23 °C for 16 h with Buffer A with no addition or with different combinations of 0.75 M TMAO and 400 $\mu$g of GroEL. After centrifugation and the collection of supernatant, the resin was washed and protein bound to the resin was eluted with Buffer A containing 200 mM imidazole. The supernatant and the imidazole-eluted fractions were analyzed by SDS-polyacrylamide gel electrophoresis.

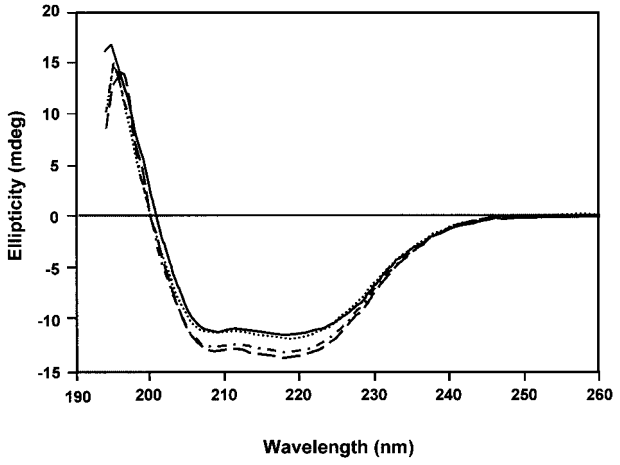


FIG. 8. **MSUD mutant E1 proteins posses folded native-like structures.** The secondary structures of wild type and mutant E1 at 0.2 mg/ml each were analyzed by CD spectroscopy as described under "Experimental Procedures." Each spectrum represents an average of three consecutive scans and is corrected for contribution from the buffer solution. The spectra are of wild type E1 (—), Y368C-$\alpha$ (...), F364C-$\alpha$ (–.–.), and Y393N-$\alpha$ (– – –) mutant E1. *mdeg*, millidegrees.

$\alpha/\beta'$ subunit interactions and results in the accumulation of heterodimers, similar to the Y393N-$\alpha$ substitution. The third member of the aromatic array Tyr-368-$\alpha$ in the E1$\alpha$ subunit is next to Gln-369-$\alpha$ that coordinates to Asn-183-$\beta$ in the E1$\beta$ subunit. The substitution of a Tyr with a Cys residue substantially weakens the $\alpha/\beta$ subunit interactions, which is essential for the integrity of the native $\alpha_2\beta_2$ heterotetramer. As a result, the Y368C-$\alpha$ mutant E1 exists as both heterodimers and heterotetramers.

Organic osmolytes including TMAO are capable of forcing otherwise naturally unstructured proteins such as AF1/tau1 domain of the glucocorticoid receptor (15, 16) and reduced/carboxyamidated ribonucleases (17, 18) to fold *in vitro*. TMAO was also shown to protect against urea-induced dissociation and inactivation of lactate dehydrogenase *in vitro* (32). TMAO promotes protein folding by preferential hydration of the exposed peptide backbone of an unfolded protein (33). This produces a thermodynamically unstable state associated with the increased ordering of bound water molecules. This entropically unfavorable situation promotes the folding of the unfolded protein into a native conformation, in which exposed side chains

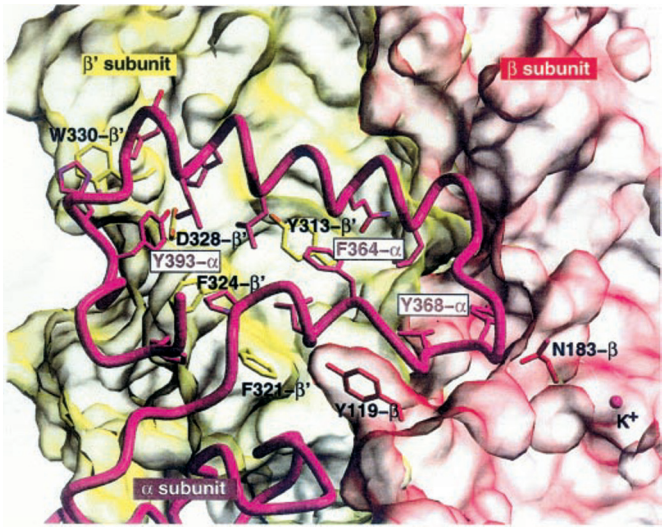


FIG. 9. **Type IA MSUD mutations in the Mennonite region impede interactions of the $\alpha$ subunit with the $\beta$ or $\beta'$ subunit.** The C-terminal domain of E1$\alpha$ subunit shown as a coil backbone is packed against semitransparent surfaces of the $\beta$ (*red*) and $\beta'$ (*yellow*) subunits. Selected side chains are marked, and the three aromatic residues, Tyr-393-$\alpha$, Phe-364-$\alpha$, and Tyr-368-$\alpha$, that are affected in MSUD are *highlighted*. This segment of the E1$\alpha$ chain is called the Mennonite region, because of the presence of the prevalent Y393N-$\alpha$ mutation in this population. Tyr-393-$\alpha$ is hydrogen-bonded to Asp-328-$\beta'$ in the $\beta'$ subunit. Phe-364-$\alpha$ is packed against Tyr-313-$\beta'$ also in the $\beta'$ subunit. Tyr-368-$\alpha$ is packed against the $\beta$ subunit at the $\alpha/\beta$ subunit interface. Reproduced from Ævarsson *et al.* (8) with permission.

are sequestered and the osmolyte is excluded from the peptide backbone. Therefore, the Gibbs free energy of the native conformation is significantly lower than that of the TMAO-bound unfolded ensemble.

Although TMAO-facilitated protein folding has been studied at length, much less is known concerning the effects of the osmolyte on protein assembly. TMAO was shown to enhance the assembly and stability of microtubules (34) and accelerate fibril assembly in the amyloid-$\beta$ aggregation pathway (35). It is suggested that the same preferential hydration effect of TMAO promotes protein oligomerization. In the present study, we extend this concept by showing that TMAO corrects protein assembly defects caused by MSUD mutations after folding. As a case in point, the Y393N-$\alpha$ mutation abolishes interactions between $\alpha\beta$ and $\alpha'\beta'$ heterodimers at the $\alpha/\beta'$ and $\alpha'/\beta$ subunit interfaces. It is possible that TMAO mitigates this impairment by destabilizing the folded Y393N-$\alpha$ heterodimers through hydration. The resultant increase in Gibbs free energy in the mutant heterodimer forces its association with another TMAO-bound heterodimer. The hydration effect of TMAO may further force the two loosely associated mutant heterodimers to form a tighter packing along the defective $\alpha/\beta'$ and $\alpha'/\beta$ subunit interfaces, resulting in an entropically more stable mutant heterotetramer. TMAO-mediated hydration exerts little, if any, effects on the wild type heterotetramer, because it is already in the most stable native conformation. In the presence of physiological E2 or TPP, the active heterotetrameric conformation of the mutant E1 is largely maintained even after the removal of the osmolyte. The stabilization effect of bound ligands was also observed with the TMAO-induced folded structure of the AF1/tau1 domain in the glucocorticoid receptor (16).

The expression and assembly of wild type and MSUD mutant E1 proteins is absolutely dependent on the coexpression of the chaperonins GroEL/GroES (10, 36). The assembly of the wild type E1 $\alpha_2\beta_2$ heterotetramer proceeds through an $\alpha\beta$ heterodimeric intermediate, which presumably represents an ensemble of low energy valleys in the folding energy landscape. In

the presence of Mg-ATP, these bacterial chaperonins convert trapped wild type E1 heterodimeric intermediate to its productive counterpart, capable of forming heterotetramers, through iterative dissociation/reassociation cycles (30, 31). Interactions of the GroEL double-ring complex with the 86-kDa heterodimeric intermediate occurs in the *cis* cavity capped by GroES (31). However, GroEL/GroES are unable to rescue trapped heterodimers dictated by the type IA MSUD mutations, either in *E. coli* (10) or during *in vitro* refolding (25). The results are consistent with the concept that molecular chaperones promote protein folding but do not contain steric information that determines the final protein structure (37).

During chaperonins GroEL/GroES-mediated *in vitro* refolding, the recovered activity of Y368C-$\alpha$ mutant E1 is 17-fold higher in the presence of TMAO than in its absence. In contrast, TMAO has no effect on the renatured wild type E1 activity under similar conditions. Delayed additions of TMAO for up to 6 h during refolding of Y368C-$\alpha$ mutant E1 does not affect the activation of E1 activity by the osmolyte (data not shown). These findings suggest that the TMAO exerts its effects after the mutant E1 is folded and trapped in the heterodimeric conformation. Therefore, chaperonins and TMAO work in tandem to enhance the recovery of enzyme activity during refolding of mutant E1. Interestingly, TMAO causes the aggregation of wild type glutamine synthetase during *in vitro* refolding, and it has been suggested that the compactness of the folded monomer in the presence of osmolyte is the reason for its failure to assemble into a functional oligomer (38). Chaperonins GroEL/GroES promote the dissociation of trapped heterodimers, and the separated $\alpha$ and $\beta$ monomers reassociate to form "good" heterodimers capable of spontaneous dimerization (30). In contrast to this mechanism, TMAO achieves the conversion of trapped mutant E1 heterodimers to heterotetramers without promoting dissociation of the mutant heterodimers. The transformation from heterodimers to heterotetramer by either chaperonins (25) or TMAO (present study) exhibits rather slow kinetics. The results are similar to those observed during the TMAO-assisted renaturation of the mutant $\Delta$468 glutamine synthetase (19) and amyloid-$\beta$ assembly in the presence of TMAO (35).

The beneficial effects of TMAO on the clinical phenotypes of certain genetic diseases have been demonstrated at the cell culture level. For example, TMAO at 100 mM has been shown to reverse defective trafficking of $\Delta$F508 cystic fibrosis transmembrane conductance regulator (20) and enhance antigen presentation in antigen-presenting cells (39). A serum concentration of 50 mM TMAO with a long half-life of 18–21 h has been achieved in a mouse model (40). These findings offer an auspicious prospect for the use of chemical chaperones such as TMAO as an approach to eradicate human diseases caused by protein misfolding. The results presented in this study demonstrate for the first time that the TMAO is capable of correcting assembly defects associated with MSUD after folding and at the step of the trapped heterodimeric ensemble. Whether these *in vitro* results have direct application in the treatment of MSUD patients will be addressed by cell culture studies.

REFERENCES


1. Chuang, D. T., and Shih, V. E. (2001) in *The Metabolic and Molecular Basis of Inherited Disease* (Scriver, C. R., Beaudet, A. L., Sly, W. S., and Valle, D., eds) 8th Ed., pp. 1971–2005, McGraw-Hill Book Co., New York
2. Menkes, J. H., Hurst, P. L., and Craig, J. M. (1954) *Pediatrics* **14,** 462–467
3. Scriver, C. R., MacKenzie, S., Clow, C. L., and Delvin, E. (1971) *Lancet* **1,** 310–312
4. Taylor, J., Robinson, B. H., and Serwood, W. G. (1978) *Pediatr. Res.* **12,** 60–62
5. Pettit, F. H., Yeaman, S. J., and Reed, L. J. (1978) *Proc. Natl. Acad. Sci. U. S. A.* **75,** 4881–4885
6. Reed, L. J., Damuni, Z., and Merryfield, M. L. (1985) *Curr. Top. Cell. Regul.* **27,** 41–49
7. Harris, R. A., Paxton, R., Powell. S. M., Goodwin, G. W., Kuntz, M. J., and Han, A. C. (1986) *Adv. Enzyme Regul.* **25,** 219–237
8. Ævarsson, A., Chuang, J. L., Wynn, R. M., Turley, S., Chuang, D. L., and Hol, W. G. J. (2000) *Structure* **8,** 277–291
9. Lindqvist, Y., Schneider, G., Ermler, U., and Sundstrom, M. (1992) *EMBO J.* **11,** 2373–2379
10. Wynn, R. M., Davie, J. R., Chuang, J. L., Cote, C. D., and Chuang, D. T. (1998) *J. Biol. Chem.* **273,** 13110–13118
11. Fisher, C. R., Fisher, C. W., Chuang, D. T., and Cox, R. P. (1991) *Am. J. Hum. Genet.* **49,** 429–434
12. Matsuda, I., Nobukuni, Y., Mitsubuchi, H., Indo, Y., Endo, F., Asaka, J., and Harada, A. (1990) *Biochem. Biophys. Res. Commun.* **172,** 646–651
13. Forster, R. P., and Goldstein, L. (1976) *Am. J. Physiol.* **230,** 925–931
14. Wang, A., and Bolen, D. W. (1997) *Biochemistry* **36,** 9101–9108
15. Baskakov, I. V., Kumar, R., Srinivasan, G., Ji, Y. S., Bolen, D. W., and Thompson, E. B. (1999) *J. Biol. Chem.* **274,** 10693–10696
16. Kumar, R., Lee, J. C., Bolen, D. W., and Thompson, E. B. (2001) *J. Biol. Chem.* **276,** 18146–18152
17. Baskakov, I., and Bolen, D. W. (1998) *J. Biol. Chem.* **273,** 4831–4834
18. Qu, Y., Bolen, C. L., and Bolen, D. W. (1998) *Proc. Natl. Acad. Sci. U. S. A.* **95,** 9268–9273
19. Voziyan, P. A., Jadhav, L., and Fisher, M. T. (2000) *J. Pharm. Sci.* **89,** 1036–1045
20. Brown, C. R., Hong-Brown, L. Q., Biwersi, J., Verkman, A. S., and Welch, W. J. (1996) *Cell Stress Chaperones* **1,** 117–125
21. Tatzelt, J., Prusiner, S. B., and Welch, W. J. (1996) *EMBO J.* **15,** 6363–6373
22. Burrows, J. A., Willis, L. K., and Perlmutter, D. H. (2000) *Proc. Natl. Acad. Sci. U. S. A.* **97,** 1796–1801
23. Welch, W. J., and Brown C. R. (1996) *Cell Stress Chaperones* **1,** 109–115
24. Chuang, J. L., Davie, J. R., Chinsky, J. M., Wynn, R. M., Cox, R. P., and Chuang D. T. (1995) *J. Clin. Invest.* **95,** 954–963
25. Chuang, J. L., Wynn, R. M., Song, J. L., and Chuang, D. T. (1999) *J. Biol. Chem.* **274,** 10395–10404
26. Wynn, R. M., Davie, J. R., Song, J. L., Chuang, J. L., and Chuang, D. T. (2000) *Methods Enzymol.* **324,** 179–191
27. Chuang, J. L., Davie, J. R., Wynn, R. M., and Chuang, D. T. (2000) *Methods Enzymol.* **324,** 192–200
28. Wynn, R. M., Ho, R., Chuang, J. L., and Chuang, D. T. (2001) *J. Biol. Chem.* **276,** 4168–4174
29. Wynn, R. M., Chuang, J. L., Sansaricq, C., Mandel, H., and Chuang, D. T. (2001) *J. Biol. Chem.* **276,** 36550–36556
30. Wynn, R. M., Song, J. L., and Chuang, D. T. (2000) *J. Biol. Chem.* **275,** 2786–2794
31. Song, J. L., Wynn, R. M., and Chuang, D. T. (2000) *J. Biol. Chem.* **275,** 22305–22312
32. Baskakov, I., and Bolen, D. W. (1998) *Biophys. J.* **74,** 2658–2665
33. Lin, T. Y., and Timasheff, S. N. (1994) *Biochemistry* **33,** 12695–12701
34. Sackett, D. L. (1997) *Am. J. Physiol.* **273,** R669–R676
35. Yang, D. S., Yip, C. M., Huang, T. H. J., Chakrabartty, A., and Fraser, P. E. (1999) *J. Biol. Chem.* **274,** 32970–32974
36. Wynn, R. M., Davie, J. R., Cox, R. P., and Chuang, D. T. (1992) *J. Biol. Chem.* **267,** 12400–12403
37. Ellis, R. J, and van der Vies, S. M. (1991) *Annu. Rev. Biochem.* **60,** 321–347
38. Voziyan, P. A., and Fisher, M. T. (2000) *Protein Sci.* **9,** 2405–2412
39. Ghumman, B., Bertram, E. M., and Watts, T. H. (1998) *J. Immunol.* **161,** 3262–3270
40. Bai, C., Biwersi, J., Verkman, A. S., and Matthay, M. A. (1998) *J. Pharmacol. Toxicol. Methods* **40,** 39–45